Online Kron Reduction for Economical Frequency Control of Microgrids

Babak Abdolmaleki, *Member*, and Qobad Shafiee, *Senior Member*

***Abstract*—Herein, a distributed switched control system is proposed which aims at frequency regulation and total generation cost minimization within a droop-based microgrid considering generator and line power constraints. The minimization is solved with Lagrange method and is achieved by realizing the equal incremental cost criterion via consensus algorithm. An online network reconfiguration is also proposed which bypasses a distributed generator when it violates the generation limits or gets disconnected, or when its corresponding line power flow exceeds its upper limit. It is mathematically probed that the proposed reconfiguration is a distributed online Kron reduction which leads to a new reduced data network; it preserves the existing spanning trees from cutting when a distributed generator is bypassed. Equilibrium analyses are conducted to show that the proposed switched system converges to the desired steady state. The stability of the system based on common quadratic the Lyapunov function is discussed. The effectiveness of the proposed controller for different case studies is verified by adapting it to a test microgrid system.**

***Index Terms*—Economic dispatch, frequency control, microgrid, Kron reduction, plug and play, secondary control.**

NOMENCLATURE

δ_i, f_i	Phase angle & frequency.
V_i, V_i^{ref}	Capacitor voltage & its reference.
f^*, V^*	Rated frequency & voltage.
P_i^m, Q_i^m	Measured active & reactive powers.
P_i, Q_i	Actual active & reactive powers.
P_i^*, Q_i^*	Rated active & reactive powers.
τ_i^V, τ_i^{LP}	First-order filters' time constants.
m_i, n_i	Droop coefficients.
$\overline{\Delta f}, \overline{\Delta V}$	Maximum allowable deviations.
$\alpha_i, \beta_i, \gamma_i$	Nonnegative cost function coefficients.
$P_{\text{load}}, P_{\text{loss}}$	MG's load power & power loss.
$P_i^{\min}, P_i^{\max}$	DG's minimum, maximum generation limits.
$P_{kl}, P_{kl}^{\max}$	Line power flow from bus l to bus k & its limit.
$P_{i-kl}^{\max}$	DG power where $P_{kl}(P_{i-kl}^{\max}) = P_{kl}^{\max}$.
$s_i, s_i^{\text{DG}}, s_i^{kl}$	ED problem logical indicators.
$s_i^{\min}, s_i^{\max}$	ED problem logical indicators.
λ	ED problem Lagrange multiplier.
$\frac{\partial C_i(P_i)}{\partial P_i}$	Incremental cost.
$\delta f_i, \Omega_i$	Frequency correction & secondary variable.
$g_i^\Omega, g_i^y, g_i^{\text{line}}$	Positive feedback gains.
$u_i^y, u_i^{\text{line}}, h_i^{kl}$	Switching inputs (signals).
y_i	i^{th} DG's forwarded data to its out-neighbors.
λ_i	i^{th} DG's secondary control variable.
Γ_i	Average of i^{th} DG's in-neighbors data.
a_{ij}, d_i, d_i^o	Link weighting & degrees. See Section II-A.
N_i, N_i^o	Neighbor sets. See Section II-A.
N_i^{line}	Line neighbor set. $N_i^{\text{line}} = \{kl \vert \frac{\partial P_{kl}}{\partial P_i} > 0\}$.
$\mathcal{L}, \mathcal{D}, \mathcal{A}$	Communication matrices. See Section II-A.
$\mathcal{N}$	Set of all the n DGs.
$\mathcal{N}_N, n_N$	Set of DGs in Normal mode & its cardinality.
$\mathcal{N}_F, n_F$	Set of DGs in DG Fail mode & its cardinality.
$\mathcal{N}_{DV}, \mathcal{N}_{LV}$	Sets of DGs in DG & Line Violated modes.
n_{DV}, n_{LV}	Cardinalities of the sets $\mathcal{N}_{DV}, \mathcal{N}_{LV}$.
k_i^y	$k_i^y \vert_{d_i=0} = 0$ & $k_i^y \vert_{d_i \neq 0} = 0.5 g_i^y m_i \alpha_i^{-1} d_i^{-1}$.
$\mathbf{k}_{n_x}^y$	Diagonal matrix $\text{diag}\{k_i^y\}, \forall i \in \mathcal{N}_x$.
$\mathbf{g}_{n_x}^\Omega, \mathbf{g}_{n_x}^y$	Matrices $\text{diag}\{g_i^\Omega\}$ & $\text{diag}\{g_i^y\}, \forall i \in \mathcal{N}_x$.
$\mathbf{g}_{n_x}^{\text{line}}, \mathbf{m}_{n_x}$	Matrices $\text{diag}\{g_i^{\text{line}}\}$ & $\text{diag}\{m_i\}, \forall i \in \mathcal{N}_x$.
$\mathbf{\Omega}_{n_x}, \boldsymbol{\lambda}_{n_x}$	Column vectors $\text{col}\{\Omega_i\}$ & $\text{col}\{\lambda_i\}, \forall i \in \mathcal{N}_x$.
$\mathbf{f}_{n_x}, \mathbf{P}_{n_x}$	Vectors $\text{col}\{f_i\}$ & $\text{col}\{P_i\}, \forall i \in \mathcal{N}_x$.
$\mathbf{P}_{n_x}^{\text{limit}}, \mathbf{u}_{n_x}^{\text{line}}$	Vectors $\text{col}\{P_i^{\text{min/max}}\}, \text{col}\{u_i^{\text{line}}\}, \forall i \in \mathcal{N}_x$.
$\mathbf{V}, \boldsymbol{\delta}, \boldsymbol{\delta f}$	Vectors $\text{col}\{V_i\}$, $\text{col}\{\delta_i\}$, & $\text{col}\{\delta f_i\}, \forall i \in \mathcal{N}$.
$\boldsymbol{\lambda}, \mathbf{Q}_m, \mathbf{P}_m$	Vectors $\text{col}\{\lambda_i\}$, $\text{col}\{Q_i^m\}$, $\text{col}\{P_i^m\}, \forall i \in \mathcal{N}$.
$\mathbf{x}_{\text{drp}}$	$[\mathbf{Q}_m^T \ \mathbf{P}_m^T \ \mathbf{V}^T \ \boldsymbol{\delta}^T]^T$: MG state vector.
$\mathbf{w}_{\text{drp}}, \mathbf{A}_{\text{drp}}$	Droop-based MG disturbances & state matrix.
$\mathbf{w}_\lambda^\xi, \mathbf{A}_\lambda^\xi$	Disturbances & state matrix of SFC.
$\sigma_{\min}^{\mathcal{Q}}, \sigma_{\max}^{\mathcal{Q}}$	Minimum & maximum eigenvalues of $\mathcal{Q}$.
τ	Communication delay.

The authors are with the Smart/Micro Grids Research Center, University of Kurdistan, Sanandaj, Iran (e-mail: abdolmaleki.p.e@gmail.com; q.shafiee@uok.ac.ir).

I. INTRODUCTION

TO stably integrate multiple grid-forming distributed generators (DGs) into the islanded microgrids (MGs) *droop control* is a communication-free custom [1], [2]. Despite its simple, low-cost, and plug-and-play functionality, the conventional droop control leads to frequency deviation and does not ensure an economical inter-DG power-sharing. These concerns could be addressed by employing some frequency restoration and economic power-sharing schemes under the umbrella of MGs' hierarchical control policy [3]. Frequency restoration should occur with a feasible power formation. This frequency-power control scheme is also known as **S**econdary **F**requency **C**ontrol (**SFC**). On the other hand, minimization of the DGs' total generation cost, known as **E**conomic **D**ispatch (**ED**), is mandatory for long-term cost-effective operation of power systems [4]. To solve the SFC and ED problems for MGs, different centralized, decentralized, and distributed methods have been proposed in the literature. In the centralized methods the DGs information is all gathered and synthesized in a central unit and then, appropriate commands are sent back

to the DGs. These methods are not scalable, require a costly, complex communication infrastructure, and exhibit a single point of failure [5], [6]. Next, the literature concerning *non-centralized* SFC/ED methods applied to islanded MGs are surveyed.

A. Literature Review

1) ***Secondary frequency control (SFC):*** Decentralized SFC of MGs has been investigated in [7]–[12]. These controllers require no communications, but they may rely on some signal-processing-based change detection techniques [7], [8] and propose an occasional frequency restoration, or rely on some filter-based droop coefficients [9]–[12] and introduce a trade-off between restoration speed and power-sharing tasks.

Compared with decentralized methods and as a result of inter-DG information flow through communication links, distributed SFC presents a faster and more accurate performance. Among different distributed approaches, the consensus-based SFC schemes using neighbor-to-neighbor communications [13]–[37] are preferred to the methods utilizing all-to-all communications [38]–[40] in terms of expandability and infrastructure's cost (by using sparse communication links).

In [13]–[16], some similar consensus-based SFC is proposed which utilizes the leader-following (resp. average) consensus algorithm [41], [42] for frequency (resp. active power) control. Over time, the performance of this SFC has been modified by using, e.g., finite-time [17], [18], robust [19], adaptive [20], noise-resilient [21], optimal [22], and event-triggered [23] control techniques. Semi-similar to [13]–[16] a SFC for droop-based MGs is proposed in [24]. In order to gain faster convergence and bounded frequencies, the work in [24] has been modified by using some finite-time bounded control techniques in [25], [26]. On the whole, the SFCs in [13]–[26] are all based on *defining* auxiliary control inputs such that the SFC problem is considered as cooperative control of a first-order, two-variable multi-agent system (MAS). However, the frequency and active power have algebraic relation through the droop equation. Therefore, this consideration gives a *dummy* MAS model and some unrealistic theoretical analyses. These concerns do not exist in the works [27]–[37]. In [27], first the frequency drop is eliminated by adding itself to the droop equation, and then a finite-time consensus-based SFC is proposed. A cooperative SFC is proposed in [28] with the DGs' frequencies and frequency correction terms being the exchanged data. Performance of this controller has been improved in [29] by using a robust finite-time sliding-mode control scheme.

In all the mentioned works in [13]–[29], it is assumed that only a few numbers of the DGs are aware of the frequency reference; hence, the leader-following consensus algorithm is employed for frequency tracking control. In power systems, the DGs' frequencies can reach consensus per se. Hence, a leader-following consensus-based frequency control seems to be redundant. On the contrary, in [30]–[37], the frequency restoration task is implemented locally while the consensus algorithm is only dedicated to power-sharing control. In [30]–[35], each DG is augmented with an proportional-interal (PI) controller eliminating the steady-state frequency error and providing the consensus of the frequency correction terms. In order to compensate for the frequency deviations equally, in [36] the average of the frequency drops is added to the droop equations as correction terms. Therein, this average value is computed by using a *dynamic consensus* algorithm [43], distributively. To remove the need for a PI-controller, an instantaneous event-triggered frequency control is proposed in [37]. In this scheme, the average of the frequency deviations of neighboring DGs is added to the frequency droop control as a correction term.

2) ***Economic dispatch (ED):*** In [44], a nonlinear droop scheme with consideration of the cost functions for parameters of interest is proposed which ensures that the most costly DG produces the least power. To achieve more economical operation, in [45], the droop coefficients of the conventional droop control are prioritized economically. In this work, some nonlinear droop coefficients are also proposed to widen the operational ranges of the proposed cost-prioritized droop control. In [46], [47], to avoid the complexity of the above nonlinear droop controllers, some economically tuned droop coefficients are proposed which account for the DGs' operational limits. In the works [44]–[47], however, the proposed schemes do not minimize the MG's *total* generation cost. In [48], a nonlinear droop control is proposed parameters of which are tuned by using a heuristic optimization algorithm trying to minimize MG's total generation cost based on all the DGs' information. In [49], the method in [48] is extended to a plug-and-play optimization scheme. Some droop controls are proposed in [3], [50], [51] where the frequency drop is proportional to the derivative of each DG's cost function. Hence, these cost-based droop controls realize the **E**qual **I**ncremental **C**ost **(EIC)** criterion in steady state which is the condition for first-order optimality of the DGs total generation cost [4]. The above methods yield frequency deviations and some of them do not optimize the total generation cost accurately or do not account for generation and line power flow limits.

On top of the decentralized ED methods, there are several distributed ones in the literature [17], [52]–[56]. In [52], a discrete consensus-based approach is proposed to solve the ED problem in power systems distributively. The impacts of the communication delays on the performance and design of this ED method is investigated in [53]. In order to achieve speedy convergence, the method in [52] is augmented with a distributed minimum-time algorithm in [54]. In [17], a continuous-time consensus-based ED is proposed providing the DGs with optimal power references. Finite-time convergence and delay effects associated with the ED in [17] are investigated in [55] and [56], respectively. Note that the methods in [17], [52]–[56] are implemented as *tertiary controls*, utilize load measurements/estimations to solve the ED problem, consider the power limits as *inequality constraints*, and do not consider the line power flow constraints.

3) ***Simultaneous SFC and ED:*** A decentralized SFC and ED is proposed in [57] by using low-pass filters and hence there exists a trade-off between its accuracy and convergence speed. Ref. [3] was the first to establish the connection between droop control, SFC, and minimization of a quadratic

cost function, where the proportional power-sharing is considered as an ED problem and then an average consensus-based SFC is proposed. A distributed SFC-ED is proposed in [58] where the frequencies and incremental costs are regulated via the leader-following and average consensus algorithms, respectively. In [59], a consensus-based ED scheme is proposed to tune the droop coefficient of the cost-based droop control proposed in [50]. In this work, the SFC in [31] is also employed to compensate for the frequency deviations. The SFC and ED in this work, however, are implemented through two separate consensus algorithms. A gather-and-broadcast SFC is proposed in [60] where the optimal incremental costs are *centrally* computed and then, they are translated into frequency correction terms distributively.

B. Contributions and Paper Outline

In addition to the sparsely mentioned inadequacies in the previous subsection, the major gaps within the literature are as follows. *i)* None of the works in Section I-A1 accounts for economic operation of MGs, *ii)* the works in Section I-A2 are primary or tertiary controllers and do not address frequency deviations, and *iii)* the works in Section I-A3 are based on the cost-based droop controls in [50] instead of the conventional droop control, do not account for line power flow limits, and except for [59] do not account for generation limits. In this paper, inspired by the surveyed literature and motivated by the above statements, a distributed SFC-ED scheme is proposed with the following contributions.

C1: The ED optimization problem considering the DGs power limits, plug-and-play ability, and line power flow constraints is formulated first. Then, a *consensus-based* correction term, based on *general directed communication network graphs*, is introduced which eliminates the droop-induced frequency deviations and realizes the equal incremental cost principle. The proposed controller is single-state and under this scheme only one data is communicated between the DGs.

C2: A *switched control system* is proposed which *i)* realizes the incremental costs consensus for the DGs that work within power limits, *ii)* commands the DGs to inject maximum, minimum, or zero power when they violate the limits or get disconnected, and *iii)* tunes the DGs power such that their corresponding line power flow remain at its maximum value. The system equilibrium depends on the existence of a *spanning tree* within the communication network graph. Therefore, a distributed *online network reconfiguration* is proposed which preserves the spanning trees within the communication graph from cutting, by *eliminating* or *bypassing* the DG from the economic dispatch problem in the following situations. *i)* When a DG *does not work within power limits*, *ii)* when a DG *gets disconnected temporarily*, or *iii)* when a DG's corresponding line power flow exceeds its upper limit.

C3: Mathematical Kron reduction, equilibrium, and stability analyses are conducted to show the effectiveness of the proposed control system. It is mathematically probed that the proposed reconfiguration is an *online Kron reduction* leading to a *reduced communication network* among the DGs working within power limits. Please, note that prior to this, Kron reduction strategy has been applied to the large scale systems in *offline* analyses to reduce their dimensions [61]. To the authors knowledge, there is no suitable alternative to bypass a node within the communication network in an *instantaneous*, *online* manner.

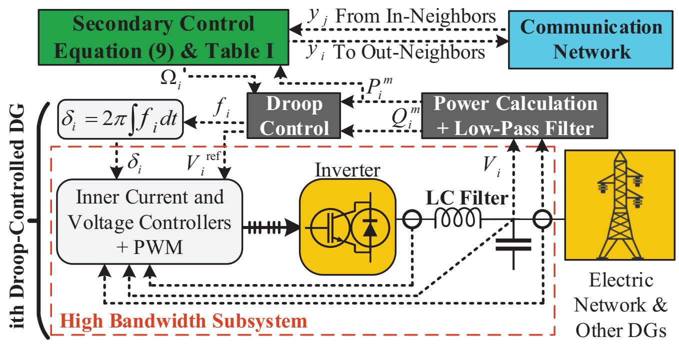

Fig. 1. Schematic of a droop-based MG with the proposed controller.

The reminder of this paper is structured as follows. Section II provides the system modeling and describes the control tasks. The switched frequency controller is introduced and elaborated in Section III. Simulation results verifying the effectiveness of the controller are presented in Section IV. Finally, Section VI concludes the paper.

II. System Setup

A. Communication Network (CN) and Graph Theory

The CN among the DGs, can be regarded as a directed graph (digraph) with the DGs and communication links playing the roles of its nodes and edges, respectively. Consider the graph $\mathcal{G} = (\mathcal{N}, \mathcal{E}, \mathcal{A})$, where $\mathcal{N} = \{1, ..., n\}$, $\mathcal{E} \subseteq \mathcal{N} \times \mathcal{N}$, and $\mathcal{A} = [a_{ij}] \in \mathbb{R}^{n \times n}$ are its node set, edge set, and adjacency matrix, respectively. If node i directly obtains data from node j, then, node j is an in-neighbor (sender) of node i, node i is an out-neighbor (receiver) of node j, $(j, i) \in \mathcal{E}$, and $a_{ij} = 1$; otherwise, nodes i and j are not neighbors, $(j, i) \notin \mathcal{E}$, and $a_{ij} = 0$. Let $N_i = \{j \mid (j, i) \in \mathcal{E}\}$, $N_i^o = \{j \mid (i, j) \in \mathcal{E}\}$, $d_i = \sum_{j \in N_i} a_{ij}$, and $d_i^o = \sum_{j \in N_i^o} a_{ji}$ be the in-neighbor set, out-neighbor set, in-degree, and out-degree of node i, respectively. Laplacian matrix of $\mathcal{G}$ is $\mathcal{L} = \mathcal{D} - \mathcal{A}$, where $\mathcal{D} = \text{diag}\{d_i\}$. A directed path from node j to node i is a sequence of pairs, belong to $\mathcal{E}$, expressed as $\{(j, n_1), ..., (n_m, i)\}$. A graph has a spanning tree, if there is a node r (called the root node), such that there is a directed path from the root node to every other node in the graph [41]–[43], [62].

B. Droop-Controlled Inverter-Based Microgrids

Under the hierarchical control structure, the most inner controllers are responsible to control the LC filter's inductor current and capacitor voltage. Up to now, various types of the inner controllers have been proposed, e.g., PI-based [2], PR-based [63], sliding mode [64], and model predictive [65] controllers. In addition, these controllers are normally designed to be very fast such that the subsystem denoted by red dashed lines in Fig.1 has a very high bandwidth. Hence,

generally one can use the following first order state model for i^{th} *inverter-interfaced DG* in secondary control design and stability analyses [28], [66].

$$\dot{\delta}_i = 2\pi f_i, \tag{1a}$$
$$\tau_i^V \dot{V}_i = -V_i + V_i^{\text{ref}}. \tag{1b}$$

In MGs with inductive (actual or virtual) line impedances, active and reactive powers are dominantly affected by frequency and voltage, respectively. Thus, the droop mechanism can be used to tune i^{th} inverter-interfaced DGs' output frequency and voltage as follows [18].

$$f_i = f^* - m_i P_i^m, \quad m_i = \overline{\Delta f}/P_i^*, \tag{2a}$$
$$V_i^{\text{ref}} = V^* - n_i Q_i^m, \quad n_i = \overline{\Delta V}/Q_i^*. \tag{2b}$$

P_i^m, Q_i^m are the measured by using the low-pass filters below.

$$\tau_i^{LP}\dot{P}_i^m = -P_i^m + P_i(\delta_1, \cdots, \delta_n, V_i, \cdots, V_n), \tag{3a}$$
$$\tau_i^{LP}\dot{Q}_i^m = -Q_i^m + Q_i(\delta_1, \cdots, \delta_n, V_i, \cdots, V_n), \tag{3b}$$

P_i and Q_i are some functions of all the DGs' phase angles and voltages, reflecting power flow equations of the MG.

Remark 1: The droop control in (2), is effective only for high-voltage MGs with inductive line impedances. In resistive MGs, however, P & Q and hence f & V are highly coupled and (2) is not effective anymore. In practice, these couplings are removed by incorporating a virtual impedance loop between droop control and inner control loops such that in addition to high-voltage MGs, the droop control in (2) can be applied to low- and medium-voltage MGs. The interested reader can refer to [67] for more info on the virtual impedance concept.

The stability and equilibrium of the above described droop-based MG system have been investigated in [30], [66], [67]. Since the frequency is a global entity, in steady state one has

$$f_i = f_j = f^* - m_i P_i, \ \forall i, j, \tag{4a}$$
$$m_i P_i = m_j P_j \Rightarrow P_i/P_i^* = P_j/P_j^*, \ \forall i, j, \tag{4b}$$

This underlines the droop-induced frequency deviation and proportional power-sharing between the DGs in steady state.

C. ED Problem and EIC Principle

Let $C_i(x_i) = \alpha_i x_i^2 + \beta_i x_i + \gamma_i$ be i^{th} DG's cost function. The ED can then be formulated as the minimization problem below.

$$\min\left(\sum\nolimits_i^n C_i(P_i)\right), \begin{cases} \sum_i^n P_i = P_{\text{load}} + P_{\text{loss}}, \\ P_i^{\min} \le P_i \le P_i^{\max}, \\ P_{kl}(P_i) \le P_{kl}^{\max}, \end{cases} \tag{5}$$

Since P_{kl} and P_{lk} are considered separately, no lower limit is considered. The power flow P_{kl} (not P_{lk}) can be predominately controlled and decreased by the nearest DG to bus l, i.e., i^{th} DG. In other words, only participation factor of i^{th} DG in P_{kl} is positive, i.e., $\frac{\partial P_{kl}}{\partial P_j} \le 0, \forall j \ne i$. The above inequality-constrained ED problem can be reformulated as

$$\min\left(\sum\nolimits_i^n s_i^{\text{DG}} s_i C_i(P_i)\right), \tag{6a}$$
$$0 = P_{\text{load}} + P_{\text{loss}} - \sum\nolimits_i^n s_i^{\text{DG}} s_i P_i - \sum\nolimits_i^n s_i^{\text{DG}}(s_i^{\max} P_i^{\max} + s_i^{\min} P_i^{\min} + s_i^{kl} P_{i-kl}^{\max}), \tag{6b}$$

where

$$s_i^{\max} = \begin{cases} 1, \ P_i > P_i^{\max}, \\ 0, \ \text{otherwise}, \end{cases} \quad s_i^{\min} = \begin{cases} 1, \ P_i < P_i^{\min}, \\ 0, \ \text{otherwise}, \end{cases} \tag{6c}$$

$$s_i^{kl} = \begin{cases} 1, \ P_{kl} > P_{kl}^{\max} \text{ and } P_i^{\min} \le P_i \le P_i^{\max} \\ 0, \ \text{otherwise}, \end{cases} \tag{6d}$$

$$s_i = \begin{cases} 1, \ s_i^{\min} = s_i^{\max} = s_i^{kl} = 0, \\ 0, \ \text{otherwise}. \end{cases} \tag{6e}$$

$$s_i^{\text{DG}} = \begin{cases} 1, \ i^{\text{th}} \text{ DG is connected}, \\ 0, \ i^{\text{th}} \text{ DG is disconnected}, \end{cases} \tag{6f}$$

If i^{th} DG gets disconnected due to economic purposes or physical services, then $s_i^{\text{DG}} = 0$ and it stops injecting power and does not participate in ED as an active agent. If $P_i \in [P_i^{\min}, P_i^{\max}]$ and $P_{kl} \le P_{kl}^{\max}$, then $s_i = 1$ and i^{th} DG participates in ED actively. If $P_i \notin [P_i^{\min}, P_i^{\max}]$ or $P_{kl} > P_{kl}^{\max}$, then $s_i = 0$, and i^{th} DG is not an active agent, and injects the power of $P_i^{\min}$, $P_i^{\max}$, or $P_{i-kl}^{\max}$ (depending on $s_i^{\min}$, $s_i^{\max}$, and s_i^{kl}); hence, from other DGs viewpoint its power generation is a part of MG's power demand.

The ED optimization problem can be solved by Lagrangian method with the following Lagrangian function [4], [50].

$$\begin{aligned} L(\mathbf{P}, \lambda) = &\sum\nolimits_i^n s_i^{\text{DG}} s_i C_i(P_i) \\ &+\lambda(P_{\text{load}} + P_{\text{loss}} - \sum\nolimits_i^n s_i^{\text{DG}} s_i P_i) \\ &-\lambda\sum\nolimits_i^n s_i^{\text{DG}}(s_i^{\max} P_i^{\max} + s_i^{\min} P_i^{\min} + s_i^{kl} P_{i-kl}^{\max}). \end{aligned} \tag{7}$$

The first order optimality criterion associated with (7) are

$$\frac{\partial L}{\partial P_i} = s_i^{\text{DG}} s_i \left(\frac{\partial C_i(P_i)}{\partial P_i} - \lambda\right) = 0, \tag{8a}$$
$$\begin{aligned} \frac{\partial L}{\partial \lambda} = &-\sum\nolimits_i^n s_i^{\text{DG}}(s_i P_i + s_i^{\max} P_i^{\max} + s_i^{\min} P_i^{\min} + s_i^{kl} P_{i-kl}^{\max}) \\ &+P_{\text{load}} + P_{\text{loss}} = 0, \end{aligned} \tag{8b}$$

where $\frac{\partial C_i(P_i)}{\partial P_i} = 2\alpha_i P_i + \beta_i$. If $s_i^{\text{DG}} = 0$, then (8a) is satisfied and P_i is completely removed from the power balance equation (8b). For $s_i^{\text{DG}} = 1$, however, different cases may happen. If $s_i = 0$, then the condition (8a) is satisfied and the power of $P_i^{\min}$, $P_i^{\max}$, or $P_{i-kl}^{\max}$ (depending on $s_i^{\min}$, $s_i^{\max}$, and s_i^{kl}) is included in condition (8b) as a negative power demand. If $s_i = 1$, then (8a) is boiled down to $2\alpha_i P_i + \beta_i = \lambda$ and P_i is included in (8b). On the whole, the optimal solution is the point where

$$P_i = \begin{cases} (\lambda - \beta_i)/(2\alpha_i), & \forall i \mid s_i^{\text{DG}} s_i = 1, \\ P_i^{\min}, & \forall i \mid s_i^{\text{DG}} s_i^{\min} = 1, \\ P_i^{\max}, & \forall i \mid s_i^{\text{DG}} s_i^{\max} = 1, \\ P_{i-kl}^{\max}, & \forall i \mid s_i^{\text{DG}} s_i^{kl} = 1, \\ 0, & \forall i \mid s_i^{\text{DG}} = 0. \end{cases} \tag{8c}$$

The criterion in first case of (8c) is known as the EIC principle and is the fundamental principle for minimizing the total generation cost of the DGs with $s_i^{\text{DG}} s_i = 1$.

TABLE I
THE SWITCHING SIGNALS FOR i^{TH} DG IN (9) UNDER DIFFERENT MODES

		Signal							
		u_i^y		y_i		$a_{xi}, \forall x \in N_i^o$		h_i^{kl}	
d_i		0	+	0	+	0	+	0	+
Mode	Normal	0	u_i^1	λ_i	λ_i	1	1	0	0
	DG Violated	0	0	Nothing	Γ_i	0	1	0	0
	Line Violated	0	0	Nothing	Γ_i	0	1	1	1
	DG Fail	0	0	Nothing	Γ_i	0	1	0	0

Normal: i^{th} DG is connected and $m_i P_i^{\min} \le \Omega_i \le m_i P_i^{\max}$.
DG Violated: i^{th} DG is connected, and $\Omega_i < m_i P_i^{\min}$ or $\Omega_i > m_i P_i^{\max}$.
Line Violated: i^{th} DG is in **Normal** mode and $\exists kl \in N_i^{\text{line}} \mid P_{kl} > P_{kl}^{\max}$.
DG Fail: i^{th} DG is disconnected.

III. ECONOMICAL SECONDARY FREQUENCY CONTROL

A. Proposed Controller and Network Reconfiguration

To compensate for frequency deviations and to reach the optimal solution in (8c), the correction term δf_i is added to the droop characteristic (2a) as

$$f_i = f^* - m_i P_i^m + \delta f_i, \tag{9a}$$

$$\delta f_i = \begin{cases} m_i P_i^{\min}, & \Omega_i < m_i P_i^{\min}, \\ m_i P_i^{\max}, & \Omega_i > m_i P_i^{\max}, \\ 0, & i^{\text{th}} \text{ DG is disconnected}, \\ \Omega_i, & \text{otherwise}. \end{cases} \tag{9b}$$

The secondary control variable Ω_i, determining δf_i, is computed as follows (with the initial value of $\Omega_i(0) = m_i P_i^{\min}$).

$$\Omega_i = \int \left[g_i^{\Omega}(m_i P_i^m - \Omega_i) + g_i^y u_i^y + g_i^{\text{line}} u_i^{\text{line}} \right] dt. \tag{9c}$$

The *switching inputs* u_i^y and u_i^{line} are

$$u_i^y = \begin{cases} 0, \\ u_i^1 = 0.5 m_i \alpha_i^{-1} d_i^{-1} \sum_j a_{ij}(y_j - y_i), \end{cases}$$

$$u_i^{\text{line}} = \sum\nolimits_{kl \in N_i^{\text{line}}} h_i^{kl}(P_{kl}^{\max} - P_{kl}), \quad h_i^{kl} = \begin{cases} 1, \\ 0, \end{cases} \tag{9d}$$

where u_i^y, h_i^{kl} are selected according to Table I; y_i is defined as

$$y_i = \begin{cases} \lambda_i = 2\alpha_i m_i^{-1} \Omega_i + \beta_i \\ \Gamma_i = d_i^{-1} \sum_{j \in N_i} a_{ij} y_j, \\ \text{Nothing, i.e., } a_{xi} = 0, \forall x \in N_i^o, \end{cases} \tag{9e}$$

According to Table I, $a_{xi} \in \{0, 1\}, \forall x \in N_i^o$ and y_i takes one of the values λ_i, Γ_i, or "Nothing". Note that when "Nothing" is sent to the out-neighbors, the outgoing communication links are all interrupted, i.e., i^{th} DG sets $a_{xi} = 0, \forall x \in N_i^o$. Selection criteria of the switching signals in (9d)-(9e) are given in Table I where the operation modes are decided by using the variables Ω_i, d_i, m_i, $P_{kl}, \forall kl \in N_i^{\text{line}}$, and power limits of the DG and corresponding line(s) (see footnotes of Table I). Fig. 1 depicts schematic of a droop-based MG under the proposed controller.

B. Elaboration on the Proposed Network Reconfiguration

Consider the neighborhood-error z_i, employed in (9d) as

$$z_i = \sum a_{ij}(y_j - y_i) = -d_i y_i + a_{ik} y_k + \sum\nolimits_{j \neq k} a_{ij} y_j. \tag{10}$$

and $d_i = a_{ik} + \sum_{j \neq k} a_{ij}$. According to Section II-A, one can write (10) in the compact form $\mathbf{z} = \text{col}\{z_k\} = -\mathcal{L}\mathbf{y} \in \mathbb{R}^n$. Suppose that k^{th} DG is *not* in "Normal" mode. From Table I and (9e), one can then rewrite (10) for two cases $d_k \neq 0$ and $d_k = 0$ as follows.

*1) **Case 1** ($d_k \neq 0$):* In this case, k^{th} DG *forwards the average of its in-neighbors data*, i.e., Γ_k in (9e), to its out-neighbors; hence by substituting it for y_k in (10), the neighborhood error of other DGs can be written as

$$z_i = -d_i y_i + \sum\nolimits_{j \in N_i \& j \neq k} (a_{ij} + \frac{a_{ik} a_{kj}}{d_k}) y_j, \ \forall i, j \neq k. \tag{11}$$

Let $\mathbf{z}_{n-1} = -\mathcal{L}^1 \mathbf{y}_{n-1}$ represent compact form of (11), where $\mathbf{z}_{n-1} = \text{col}\{z_i\}$, $\mathbf{y}_{n-1} = \text{col}\{y_i\}$, $\forall i \neq k$. According to (11), one can write $\mathcal{L}^1 = \mathcal{D}^1 - \mathcal{A}^1 \in \mathbb{R}^{(n-1)\times(n-1)}$, where $\mathcal{D}^1 = \text{diag}\{d_i^1\}$, $\mathcal{A}^1 = [a_{ij}^1]$, $\forall i, j \neq k$, and

$$\begin{cases} d_i^1 = d_i = a_{ik} + \sum_{j \neq k} a_{ij}, \\ a_{ij}^1 = a_{ij} + a_{ik} a_{kj} / d_k, \qquad \forall i, j \neq k. \end{cases} \tag{12}$$

Note that for the DGs, $a_{ij}|_{j \neq k}$ in both pre-reconfiguration and post-reconfiguration communication network (CN) topology is the same, while, a_{ik} and a_{kj} only correspond with the pre-reconfiguration CN topology, which together with a_{ij} build the new communication link a_{ij}^1. According to (12), one has $d_i^1 - \sum_{j \neq k} a_{ij}^1 = 0$, where in-degree of the bypassed DG, $d_k = \sum_j a_{kj}$ is used. Hence, from Section II-A, the reduced matrix $\mathcal{L}^1$ is a Laplacian matrix for the post-reconfiguration communication network, i.e., after *bypassing* k^{th} DG. This Laplacian matrix is exactly the Kron-reduced version of the pre-reconfiguration Laplacian matrix [61]; hence the proposed reconfiguration is called *distributed online Kron reduction*. Moreover, since under the proposed strategy the *communication medium* of the bypassed DG, e.g., k^{th} DG here, interconnects the neighboring DGs (in-neighbors to out-neighbors), the data definitely finds a path to cross the bypassed DG. In other words, under the proposed strategy, any *directed path* crossing the bypassed DG is preserved. Hence, the former existing *spanning trees* comprising this directed path are also saved from cutting.

*2) **Case 2** ($d_k = 0$):* In this case, since it has *no in-neighbor*, k^{th} DG does not send data to its out-neighbors and interrupts all the data links to them, i.e., makes $a_{ik} = 0, \forall i \in N_k^o$. Hence, the neighborhood error of other DGs become

$$z_i = \sum\nolimits_{j \in N_i \& j \neq k} a_{ij}(y_j - y_i), \quad \forall i, j \neq k. \tag{13}$$

Similar to (11) and its following description, compact form of (13) is $\mathbf{z}_{n-1} = -\mathcal{L}^1 \mathbf{y}_{n-1}$ where (12) turns into

$$\begin{cases} d_i^1 = \sum_{j \neq k} a_{ij}, \\ a_{ij}^1 = a_{ij}, \qquad \forall i, j \neq k. \end{cases} \tag{14}$$

Note that for the DGs, $a_{ij}|_{j \neq k}$ in both pre-reconfiguration and post-reconfiguration communication network (CN) topology is

the same, while, a_{ik} and a_{kj} only correspond with the pre-reconfiguration CN topology and have no role in the new CN. According to (14), one has $d_i^1 - \sum_{j\neq k} a_{ij}^1 = 0$. Hence, from Section II-A, the reduced matrix $\mathcal{L}^1$ is a Laplacian matrix for the post-reconfiguration communication network, i.e., after *eliminating* k^{th} DG. On the other hand, since $d_k = 0$ one can say that *no directed path* crosses k^{th} DG in the pre-reconfiguration CN; hence, if the pre-reconfiguration CN has a spanning tree, k^{th} DG is definitely a *root node* within it. Therefore, interrupting its links to the out-neighbors, i.e., setting $a_{ik} = 0, \forall i \in N_k^o$, results in a new (reduced)sub-graph with a spanning tree rooted at one of the out-neighbors of k^{th} DG in the old network.

*3) **Results and Generalization**:* It was seen that under the proposed reconfiguration strategy, any mode change results in a new Laplacian matrix which associates with a CN among the DGs working in "Normal" mode. In the case of *consecutive mode switchings*, by applying the reconfiguration consecutively, the final reduced Laplacian matrix $\mathcal{L}^\xi \in \mathbb{R}^{n_N \times n_N}$ is obtained, where n_N denotes the number of DGs in "Normal" mode and ξ stands for ξ^{th} switching event. Moreover, the existing spanning trees are always preserved.

*4) **Justification**:* Suppose that k^{th} DG gets disconnected or touches the limits or one of its corresponding lines reaches the power limit. Since the incremental cost λ_i is a monotonic function, the other DGs should therefore reach consensus on a *new different optimal incremental cost*. If k^{th} DG does not get eliminated from the consensus algorithm, then from (10) it injects the *biased* (constant) signal y_k to its out-neighbors; acts as a *leader* for them and prevents them from reaching a new optimal point. To tackle this problem, it is conventionally assumed that in such a situation, k^{th} DG's links are *all interrupted* to eliminate it from cooperation. But, is there any guarantee for the inter-DG *information flow*, to survive this interruption? Please, take a look at Fig. 2. After interrupting the links of 2^{nd} DG, DG 1 cannot talk to DGs 3 and 4, unless 2^{nd} DG interconnects them. Under the proposed scheme, however, the data network gets *Kron-reduced* to a new network among DGs 1, 3, and 4, *instantaneously*, without any computation delay associated with 2^{nd} DG.

*5) **Responsibilities**:* Under the proposed scheme, each DG should decide *i*) which DGs to receive data from them *(in-neighbors)*, *ii*) which DGs to send data to them *(out-neighbors)*, and *iii*) *what data* to be sent. The variables in Table I, i.e., Ω_i, P_{kl}, d_i, m_i, $P_i^{\max}$, $P_i^{\min}$, and $P_{kl}^{\max}$ are locally available and the decisions are made in real time. Hence, the proposed network reconfiguration is a *distributed online Kron reduction* strategy.

C. Equilibrium Analysis

According to (3), (9) and Table I, in steady state one has

$$\mathbf{g}_{n_N}^{\Omega}(\mathbf{m}_{n_N}\mathbf{P}_{n_N} - \mathbf{\Omega}_{n_N}) - \mathbf{k}_{n_N}^{y}\mathcal{L}^\xi\boldsymbol{\lambda}_{n_N} = \mathbf{0}_{n_N}, \quad (15a)$$
$$\mathbf{g}_{n_{DV}}^{\Omega}(\mathbf{m}_{n_{DV}}\mathbf{P}_{n_{DV}} - \mathbf{\Omega}_{n_{DV}}) = \mathbf{0}_{n_{DV}}, \quad (15b)$$
$$\mathbf{g}_{n_{LV}}^{\Omega}(\mathbf{m}_{n_{LV}}\mathbf{P}_{n_{LV}} - \mathbf{\Omega}_{n_{LV}}) + \mathbf{g}_{n_{LV}}^{\text{line}}\mathbf{u}_{n_{LV}}^{\text{line}} = \mathbf{0}_{n_{LV}}, \quad (15c)$$
$$(\mathbf{f}_{n_N} - f^*\mathbf{1}_{n_N}) + (\mathbf{m}_{n_N}\mathbf{P}_{n_N} - \mathbf{\Omega}_{n_N}) = \mathbf{0}_{n_N}, \quad (15d)$$
$$(\mathbf{f}_{n_{DV}} - f^*\mathbf{1}_{n_{DV}}) + \mathbf{m}_{n_{DV}}(\mathbf{P}_{n_{DV}} - \mathbf{P}_{n_{DV}}^{\text{limit}}) = \mathbf{0}_{n_{DV}}, \quad (15e)$$
$$(\mathbf{f}_{n_{LV}} - f^*\mathbf{1}_{n_{LV}}) + (\mathbf{m}_{n_{LV}}\mathbf{P}_{n_{LV}} - \mathbf{\Omega}_{n_{LV}}) = \mathbf{0}_{n_{LV}}. \quad (15f)$$

On one hand, (15a) and (15d) correspond to [33, eq. (8)]. On the other hand, from Section III-B3, if the original inter-DG communication network has a *spanning tree*, then $\mathcal{L}^\xi$ is associated with a CN containing a spanning tree. Therefore, according to [33, Th. 2] and these equations, in steady state one has $f_i = f^*$, $m_i P_i = \Omega_i$, and $\lambda_i = \lambda_j, \forall i,j \in \mathcal{N}_N$. Hence, from (9e) one also has $\frac{\partial C_i(P_i)}{\partial P_i} = \frac{\partial C_j(P_j)}{\partial P_j}, \forall i,j \in \mathcal{N}_N$. This implies realization of the *equal incremental cost (EIC)* criterion for the DGs operating in "Normal" mode. Frequency is a global entity, i.e., $f_i = f^*, \forall i \in \mathcal{N}_{DV} \subset \mathcal{N}$. Accordingly, from (15e) one has $P_i = P_i^{\min}$ or $P_i = P_i^{\max}$, $\forall i \in \mathcal{N}_{DV}$ in steady state. Therefore, depending on the value of Ω_i, the DGs operating in "DG Violated" mode produce their minimum or maximum powers. For the same reason, one can write $f_i = f^*, \forall i \in \mathcal{N}_{LV} \subset \mathcal{N}$ and hence from (15c) and (15f) one has $m_i P_i = \Omega_i$ and $u_i^{\text{line}} = 0, \forall i \in \mathcal{N}_{LV}$. According to Table I, one can write $h_i^{kl}(P_{kl}^{\max} - P_{kl}) \leq 0$ and hence from (9d) and Table I one can say that $u_i^{\text{line}} = 0$ *if and only if* $P_{kl} \leq P_{kl}^{\max}, \forall kl \in N_i^{\text{line}}$, i.e., in steady state one has $P_{kl} \leq P_{kl}^{\max}, \forall kl \in N_i^{\text{line}}, \forall i \in \mathcal{N}_{LV}$. Altogether, one can see that the equilibrium point of the proposed control system is the optimal solution of the ED problem described by (5)-(8c).

D. Stability Analyses

State-space model of the droop-based MG in (1), (2b), and (3) under the frequency droop control in (9a) and the secondary control described in Section III-A can be written in the following compact form.

$$\dot{\mathbf{x}}_{\text{drp}} = \mathbf{A}_{\text{drp}}\mathbf{x}_{\text{drp}} + \mathbf{w}_{\text{drp}} + [\mathbf{0}_{3n}^T \; 2\pi\boldsymbol{\delta}\mathbf{f}]^T, \quad (16a)$$
$$\dot{\boldsymbol{\lambda}} = \mathbf{A}_{\lambda}^{\xi}\boldsymbol{\lambda} + \mathbf{w}_{\lambda}^{\xi} + \mathcal{F}_{\lambda}^{\xi}(\mathbf{x}_{\text{drp}}). \quad (16b)$$

$\mathcal{F}_\lambda : \mathbb{R}^{4n} \to \mathbb{R}^n$ is a nonlinear function of the droop-based MG's states. Please, note that one can can easily extract different components in (16) from (1)-(3) and (9).

From (9) and Table I, $\mathcal{N} = \mathcal{N}_N \cup \mathcal{N}_F \cup \mathcal{N}_{DV} \cup \mathcal{N}_{LV}$ and $n = n_N + n_F + n_{DV} + n_{LV}$. Hence, one can partition $\mathbf{A}_\lambda^\xi$ as

$$\mathbf{A}_\lambda^\xi = -\begin{bmatrix} \mathbf{g}_{n_N}^{\Omega} + \mathbf{g}_{n_N}^{y}\boldsymbol{\chi}_{n_N}\mathcal{L}^\xi & \mathbf{0}_{n_N\times(n-n_N)} \\ \mathbf{0}_{(n-n_N)\times n_N} & \mathbf{g}_{n-n_N}^{\Omega} \end{bmatrix}; \quad (17)$$

$\mathbf{g}_{n-n_N}^{\Omega} = \text{diag}\{g_i^{\Omega}\}, \forall i \notin \mathcal{N}_N$; $\boldsymbol{\chi}_{n_N} = \text{diag}\{\chi_i\}, \forall i \in \mathcal{N}_N$, $\chi_i|_{d_i=0} = 0$, and $\chi_i|_{d_i\neq 0} = d_i^{-1}$.

According to (9) and Table I, the sets $\mathcal{N}_N$, $\mathcal{N}_F$, $\mathcal{N}_{DV}$, and $\mathcal{N}_{LV}$ and hence $\mathbf{A}_\lambda^\xi$ and $\mathcal{F}_\lambda^\xi$ may differ in each switching event ξ. Therefore, (16b) is a *multi-mode switched linear system* [68]. One can see that each DG can possibly correspond with one of the two diagonal partitions in (17); therefore, $\mathbf{A}_\lambda^\xi$ can take $2n$ forms (modes). Next, stability of the system is analyzed.

Assumption 1: The droop-based MG system in (16a) (without considering $\boldsymbol{\delta}\mathbf{f}$), is well-designed and stable where the disturbance vector $\mathbf{w}_{\text{drp}}$ is bounded.

Fact 1: From (9b), one has $|\delta f_i| \leq \max\{m_i P_i^{\min}, m_i P_i^{\max}\}$.

Fact 2: The function $\mathcal{F}_\lambda^\xi$ is continuously differentiable and the disturbance vector $\mathbf{w}_\lambda^\xi$ comprises a set of constants and hence is bounded.

Theorem 1: Suppose that there exist the symmetric positive definite matrices $\mathcal{P}$ and $\mathcal{Q}$ such that for all possible forms of $\mathbf{A}_\lambda^\xi$ one has $(\mathbf{A}_\lambda^\xi)^T\mathcal{P}+\mathcal{P}\mathbf{A}_\lambda^\xi \leq -\mathcal{Q}, \forall\xi$. Then, under Assumption 1, Fact 1, and Fact 2, the vector $\boldsymbol{\lambda}$ is ultimately uniformly bounded.

Proof: Consider the *common quadratic Lyapunov function* [68] $\mathcal{V}(\boldsymbol{\lambda})=\boldsymbol{\lambda}^T\mathcal{P}\boldsymbol{\lambda}$. Differentiating it and considering (16b) and $\mathbf{w}=\mathbf{w}_\lambda^\xi+\mathcal{F}_\lambda^\xi(\mathbf{x}_{\text{drp}})$, one has

$$\begin{aligned}\dot{\mathcal{V}}&=\boldsymbol{\lambda}^T[(\mathbf{A}_\lambda^\xi)^T\mathcal{P}+\mathcal{P}\mathbf{A}_\lambda^\xi]\boldsymbol{\lambda}+2\boldsymbol{\lambda}^T\mathcal{P}\mathbf{w},\\&\leq -\boldsymbol{\lambda}^T\mathcal{Q}\boldsymbol{\lambda}+\tau\boldsymbol{\lambda}^T\boldsymbol{\lambda}+\tau^{-1}\mathbf{w}^T\mathcal{P}^2\mathbf{w},\\&\leq -(\sigma_{\min}^{\mathcal{Q}}-\tau)\boldsymbol{\lambda}^T\boldsymbol{\lambda}+\tau^{-1}\sigma_{\max}^{\mathcal{P}^2}\mathbf{w}^T\mathbf{w},\end{aligned}\tag{18}$$

where the inequality in Theorem 1, the well-known Young's inequality $2\boldsymbol{\lambda}^T\mathcal{P}\mathbf{w}\leq\tau\boldsymbol{\lambda}^T\boldsymbol{\lambda}+\tau^{-1}\mathbf{w}^T\mathcal{P}^2\mathbf{w}$, $\forall\tau>0$, and the inequalities $\sigma_{\min}^{\mathcal{Q}}\boldsymbol{\lambda}^T\boldsymbol{\lambda}\leq\boldsymbol{\lambda}^T\mathcal{Q}\boldsymbol{\lambda}$ and $\mathbf{w}^T\mathcal{P}^2\mathbf{w}\leq\sigma_{\max}^{\mathcal{P}^2}\mathbf{w}^T\mathbf{w}$ are used. Under Fact 1, the vector $[\mathbf{0}_{3n}^T\ \boldsymbol{\delta}\mathbf{f}^T]^T$ in (16a) can be considered as a disturbance vector and can be integrated into $\mathbf{w}_{\text{drp}}$. Therefore, one can say that the correction term δf_i does not affect the stability of the droop-controlled MG described by (16a); i.e., if Assumption 1 holds, then the system (16a) is stable. Accordingly, the state vector $\mathbf{x}_{\text{drp}}$ has bounded variations which in turn, implies that under Fact 1, the vector $\mathbf{w}=\mathbf{w}_\lambda^\xi+\mathcal{F}_\lambda^\xi(\mathbf{x}_{\text{drp}})$ is bounded, i.e., one has $\mathbf{w}^T\mathbf{w}\leq\varphi^2$. According to this inequality and (18), $\dot{\mathcal{V}}<0$ if

$$\boldsymbol{\lambda}^T\boldsymbol{\lambda}>\tau^{-1}\sigma_{max}^{\mathcal{P}^2}\varphi^2/(\sigma_{min}^{\mathcal{Q}}-\tau)=\phi^2,\tag{19}$$

implying that all the trajectories of $\boldsymbol{\lambda}$ beginning in a compact set around origin with the radius ϕ evolves completely within it. Therefore, $\boldsymbol{\lambda}$ is ultimately uniformly bounded [69]. ■

E. Eigenvalue Analyses

According to the Geršgorin discs theorem [70, Th. 6.1.1] and by using the properties of the Laplacian and in-degree matrices in Section II-A, one can say that the eigenvalues of $\mathbf{A}_\lambda^\xi$, i.e., $\sigma^{\mathbf{A}_\lambda^\xi}\in\mathbb{C}$ are located in $D_2\cup\bigcup_{i\in\mathcal{N}_N:d_i\neq0}D_1^i$ where D_1^i and D_2 are the following Geršgorin disks.

$$D_1^i=\{\sigma^{\mathbf{A}_\lambda^\xi}:|\sigma^{\mathbf{A}_\lambda^\xi}+g_i^\Omega+g_i^y|\leq g_i^y\},\begin{cases}\forall i\in\mathcal{N}_N\\ d_i\neq0,\end{cases}\tag{20a}$$

$$D_2=\{-g_i^\Omega:i\notin\mathcal{N}_N\ \text{or}\ d_i=0\}.\tag{20b}$$

It can be inferred from (20) that under positive feedback gains, all the eigenvalues of the state-matrix have negative real parts affected by g_i^Ω and g_i^y. Generally, the former determines how far the eigenvalues are centered from the imaginary axis while the latter decides how far they are dispersed from the center.

F. Time Delay Analyses

The communication delay τ affects the system through the adjacency matrix and in-neighbors data. Therefore, considering t as time argument, one can write (16b) as

$$\begin{aligned}\dot{\boldsymbol{\lambda}}_{n_N}(t)=&-(\mathbf{g}_{n_N}^\Omega+\mathbf{g}_{n_N}^y\boldsymbol{\chi}_{n_N}\mathcal{D}^\xi)\boldsymbol{\lambda}_{n_N}(t)+\mathbf{w}_{n_N}(t)\\&+\mathbf{g}_{n_N}^y\boldsymbol{\chi}_{n_N}\mathcal{A}^\xi\boldsymbol{\lambda}_{n_N}(t-\tau),\end{aligned}\tag{21a}$$

$$\dot{\boldsymbol{\lambda}}_{n-n_N}(t)=-\mathbf{g}_{n-n_N}^\Omega\boldsymbol{\lambda}_{n-n_N}(t)+\mathbf{w}_{n-n_N}(t).\tag{21b}$$

Neglecting (21b) and taking Laplace transform of (21a) (in s-domain) one has

$$\boldsymbol{\lambda}_{n_N}(s)=\frac{\mathbf{w}_{n_N}(s)+\boldsymbol{\lambda}_0}{s\mathcal{I}_{n_N}+\mathbf{g}_{n_N}^\Omega+\mathbf{g}_{n_N}^y\boldsymbol{\chi}_{n_N}(\mathcal{D}^\xi-\mathcal{A}^\xi e^{-\tau s})}.\tag{22}$$

Now, the roots of the system's characteristic quasipolynomial, i.e., $\det[\mathbf{M}(s)=s\mathcal{I}_{n_N}+\mathbf{g}_{n_N}^\Omega+\mathbf{g}_{n_N}^y\boldsymbol{\chi}_{n_N}(\mathcal{D}^\xi-\mathcal{A}^\xi e^{-\tau s})]=0$ should be analyzed. Since its determinant is zero, $\mathbf{M}$ is singular; hence, the quasipolynomial has solution *if and only if* $x^T\mathbf{M}x=0$ for some real unit-norm vector $x\in\mathbb{R}^{n_N}$ [31], i.e.,

$$\begin{aligned}&P(s)+Q(s)e^{-\tau s}=0,\\&P(s)=(x^Tx)s+x^T(\mathbf{g}_{n_N}^\Omega+\mathbf{g}_{n_N}^y\mathcal{X}_{n_N}\mathcal{D}^\xi)x,\\&Q(s)=-x^T(\mathbf{g}_{n_N}^y\mathcal{X}_{n_N}\mathcal{A}^\xi)x.\end{aligned}\tag{23}$$

The last equation corresponds to [71, eq. (2.46)]. From Section III-E, the eigenvalues of the system are all in left half plane and therefore the system is stable at $\tau=0$. The roots of (23) are continuous as a function of τ. In this way, according to the direct method in [71, Chap. 2.3.2], if at some τ, the roots of (23) cross the imaginary axis, one has $e^{j\omega\tau}=-Q(j\omega)/P(j\omega)$ resulting in (24) for $k=0,1,\cdots$ (see [71, eqs. (2.47)-(2.48)]).

$$\omega^2=\frac{(x^T\mathbf{g}_{n_N}^y\mathcal{X}_{n_N}\mathcal{A}^\xi x)^2-[x^T(\mathbf{g}_{n_N}^\Omega+\mathbf{g}_{n_N}^y\mathcal{X}_{n_N}\mathcal{D}^\xi)x]^2}{(x^Tx)^2},\tag{24a}$$

$$\omega\tau=\arg\left(\frac{x^T\mathbf{g}_{n_N}^y\mathcal{X}_{n_N}\mathcal{A}^\xi x}{jx^Tx\omega+x^T(\mathbf{g}_{n_N}^\Omega+\mathbf{g}_{n_N}^y\mathcal{X}_{n_N}\mathcal{D}^\xi)x}\right)+2k\pi.\tag{24b}$$

where $\arg(\cdot)$ denotes the argument. Now consider

$$x^T[\mathbf{g}_{n_N}^\Omega+\mathbf{g}_{n_N}^y\mathcal{X}_{n_N}(\mathcal{D}^\xi-\mathcal{A}^\xi)]x\geq0,\tag{25a}$$

$$x^T[\mathbf{g}_{n_N}^\Omega+\mathbf{g}_{n_N}^y\mathcal{X}_{n_N}(\mathcal{D}^\xi+\mathcal{A}^\xi)]x\geq0.\tag{25b}$$

If (25a) or (25b) holds, then (25) has no solution. Consequently, no poles migrate from left to right as τ varies and therefore the system is delay-independently stable. However, if neither (25a) nor (25b) holds, then (25) has a solution and only for $\tau<\tau|_{k=0}$ in (24b) the system is stable [71]. According to (25), to make the system delay-independently stable one can increase the ratio g_i^Ω/g_i^y; i.e., the more the ratio g_i^Ω/g_i^y, the more likely satisfied (25), and the more stability against communication delay.

IV. Case Studies

To verify the proposed controller's effectiveness, a 5-bus 220-V, 50-Hz microgrid powered by four DGs is simulated in MATLAB/Simscape Electrical™ environment. Fig. 2 depicts the test MG system with the data given in Table II. Herein, the PI-based controllers proposed in [63, Ch. 9] are used as inverter's inner control loops. The other parameters are as follows. $\overline{\Delta V}=11$, $\overline{\Delta f}=0.25$, $\tau_i^{LP}=1/2\pi$, $P_i^{\max}=1.2P_i^*$, $P_i^{\min}=0.2P_i^*$, $g_i^\Omega=20$, $g_i^y=5$, and $g_i^{\text{line}}=0.05$. The maximum line powers (in kW) are $P_{21}^{\max}=25$, $P_{32}^{\max}=30$, $P_{43}^{\max}=15$, $P_{54}^{\max}=40$, and $P_{15}^{\max}=25$. Moreover, one has $P_{ij}^{\max}=P_{ji}^{\max},\forall i,j$. It should be noted that each DG participates in its connected line power flow.

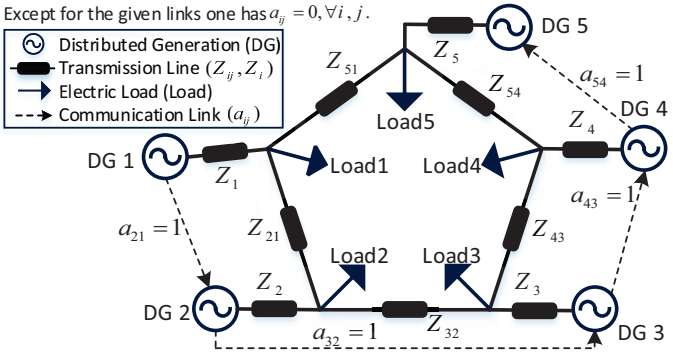

Fig. 2. Test microgrid system with the parameters given in Table II.

TABLE II
PARAMETERS OF THE TEST MICROGRID GIVEN IN FIG. 2.

DGs	DG 1	DG 2	DG 3	DG 4	DG 5
P_i^*(kW)$+jQ_i^*$(kvar)	$110+j60$	$60+j25$	$80+j45$	$75+j40$	$130+j70$
α_i	0.105	0.078	0.1	0.094	0.082
(β_i,γ_i)	(2.53,78)	(3.41,31)	(1.1,60)	(1.22,51)	(4.02,42)
Loads	Load 1	Load 2	Load3	Load 4	Load 5
P(kW)$+jQ$(kvar)	$70+j35$	$40+j20$	$35+j20$	$50+j25$	$80+j40$
DG Output Lines	Z_1	Z_2	Z_3	Z_4	Z_5
R_i+jX_i ($10^{-1}\times\Omega$)	$0.3+j0.9$	$1+j2.5$	$0.5+j1.5$	$0.8+j2.3$	$0.7+j2$
Inter-DG Lines	Z_{21}	Z_{32}	Z_{43}	Z_{54}	Z_{51}
$R_{ij}+jX_{ij}$ ($10^{-1}\times\Omega$)	$2+j3$	$1.9+j1.9$	$1.7+j2.5$	$1.5+j2.2$	$2.2+j3.2$

A. Performance of the Proposed ED and SFC Scheme

Fig. 3 indicates the system's performance under the proposed controller. Prior to $t=10s$ the MG is engaged with droop control and according to Fig. 3(a),(c), the frequencies are deviated such that the active powers are shared proportionally. After activating the controller at $t=10s$, the frequencies are all restored to 50-Hz and all the DGs' incremental costs become equal. At $t=30s$, the loads 2 and 5 increase by 35% of the MG's total load. Accordingly, the DGs increase their powers and try to keep the EIC principle. However, 2nd DG reaches its maximum power limit and therefore its power

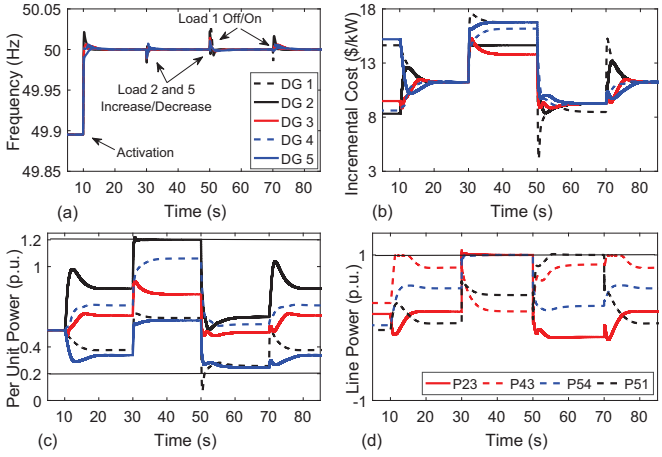

Fig. 3. Performance of the proposed controller. (a) DGs' frequencies, (b) DGs' incremental costs, (c) DGs' actual per rated active powers i.e., P_i^m/P_i^*, and (d) lines' actual per maximum active powers.

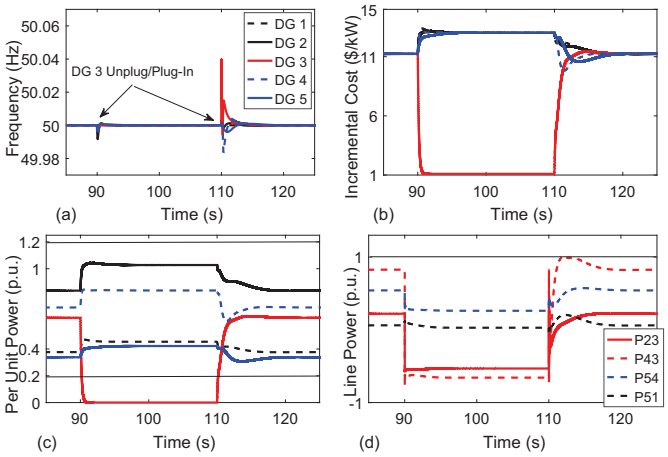

Fig. 4. Plug-and-play ability with 3rd DG. (a) DGs' frequencies, (b) DGs' incremental costs, (c) DGs' actual per rated active powers i.e., P_i^m/P_i^*, and (d) lines' actual per maximum active powers.

is set to the limit such that $P_2^m/P_2^*=1.2$. In addition, the line powers P_{23} and P_{54} arrive at their upper limits; hence, the DGs 3 and 4, which participate in P_{23} and P_{54} and are in charge of these lines, leave the incremental cost consensus task and tune their powers such that the power lines remain at their maximum values. Moreover, one can see that the other DGs which are working in normal mode, i.e., DGs 1 and 5 reach consensus on a new optimum equal incremental cost greater than the former one. It should be emphasized that from $t=30s$ to $t=50s$, 1st DG's data passes through DG 2, 3, and 4, and arrives at DG 5; therefore, the DGs 1 and 5 can reach incremental cost consensus, although their intermediate nodes are not cooperating. At $t=50s$, when loads 2 and 5 decrease to their initial values, load 1 is switched off while it is switched on again at $t=70s$. One can see that both SFC and ED problems are properly solved and the DG and line powers are kept within the reasonable limits, even after experiencing severe transient load variations. Note that the not-given line power flows have been within the reasonable range.

B. Plug-and-Play Ability

Fig. 4 indicates the plug-and-play functionality under the proposed controller. It is assumed that the MG is subjected to the proposed controller; the frequencies and the incremental costs are well-regulated. At $t=90s$, 3rd DG gets disconnected; therefore, it stops injecting power to the MG until $t=110s$ when it is connected back to the MG. It is shown that once the DG leaves the MG, other DGs produce more powers to reach incremental cost consensus. One can conclude that, the proposed controller can successfully regulate the DGs' frequencies and solves the ED problem for the connected DGs with a DG unplugged. In addition, one can see that once 3rd DG joins the MG, it immediately participates in the SFC and ED tasks.

C. System Performance Under Communication Delay

In practice, the communication delay is in the order of tens of milliseconds. However, in this part the scenario in

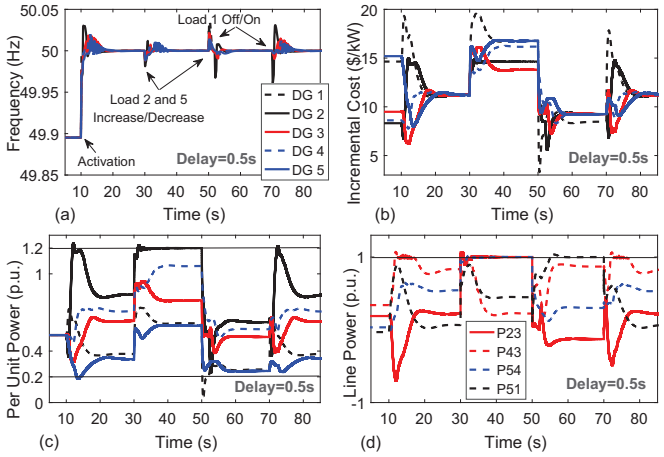

Fig. 5. Impact of communication delay on system performance. (a) DGs' frequencies, (b) DGs' incremental costs, (c) DGs' actual per rated active powers i.e., P_i^m/P_i^*, and (d) lines' actual per maximum active powers.

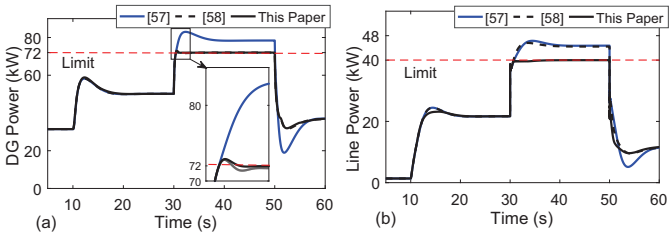

Fig. 6. System performance under different strategies. (a) 2nd DG's active power and (b) bus 4-to-bus 5 line active power.

Section IV-A under the delay of $0.5s$ is re-simulated and the results are given in Fig. 5. Comparing this figure with Fig. 3, one can see that the communication delay results in some bounded, transient overshoot and oscillations in the system responses; however, an steady-state equilibrium point same as that achieved in Section IV-A can be achieved in the presence of delay. This underlines the proposed controller's resiliency with respect to practical communication delays.

D. Comparison With the Existing Works

The scenario in the first case study is re-simulated under the proposed *distributed* controller in this paper and those in [58], [59]; 2nd DG's active power and the power flow P_{54} under different controllers are depicted in Fig. 6. According to Fig. 6(a), one can see that unlike [58], the controllers proposed in this paper and [59] can properly limit the DG's generated active power. Nevertheless, Fig. 6(b) clearly shows that only the proposed controller in this paper can account for line power flow constraints and the other two methods are not able to limit the line power flow.

V. Discussion

A simple switched control system is proposed which in the normal mode tries to realize EIC criteria by using a neighbor-to-neighbor data network. All the control actions are commanded to the droop-based DG via the only variable δf_i which is determined by using an integrator and a series of *local*, logical decisions. Indeed, the DG and line power-flow limits are accounted for by switching the control action and exchangeable data. The simulation results in Section IV-A indicate that the controller can tune the DGs' frequencies and powers such that the system's steady state is as optimum as possible in terms of EIC principle realization. In fact, the EIC realization is limited by the power generation and power flow constraints; under the proposed controller these powers are kept within the allowable ranges. This achievements are highlighted in Section IV-D by comparing the proposed controller with the other existing methods. The DGs can be temporarily disconnected for economical or maintenance-service purposes; therefore, the proposed controller can properly provide the DGs with plug-and-play ability which is studied in Section IV-B. Furthermore, the effects of communication delay on system performance is studied in Section IV-C where the system is tested under delay of 500 milliseconds although the practical delays are in the order of tens of milliseconds.

VI. Conclusion

This paper deals with solving the secondary frequency restoration and economic dispatch problems in microgrids, simultaneously. A switched control system is proposed which *i*) regulates frequency of all the DGs, *ii*) realizes the incremental costs consensus for the DGs that work within power limits, *iii*) commands the DGs to inject maximum, minimum, or zero power when they violate the limits or get disconnected, and *iv*) accounts for the line power flow constraints. The system equilibrium depends on the existence of a spanning tree within the communication network graph. Hence, an online reconfiguration strategy based on Kron reduction is proposed which bypasses the DGs within economic dispatch problem when they do not work within power limits or get disconnected temporarily. Rigorous mathematical analyses have proved the effectiveness of the proposed controller. Simulation results indicated that the proposed scheme successfully regulates the frequency of the test system and optimizes its generation cost.

Acknowledgment

The authors would like to thank Professor Florian Dörfler at Swiss Federal Institute of Technology (ETH) Zürich for his constructive comments and suggestions, which have helped enhance the presentation of the paper.

References

[1] H. Bevrani, B. François, and T. Ise, *Microgrid Dynamics and Control*. Wiely, 2017.
[2] J. Rocabert, A. Luna, F. Blaabjerg, and P. Rodríguez, "Control of power converters in AC microgrids," *IEEE Trans. Power Electron.*, vol. 27, no. 11, pp. 4734–4749, Nov. 2012.
[3] F. Dörfler, J. W. Simpson-Porco, and F. Bullo, "Plug-and-play control and optimization in microgrids," in *Proc. 53rd IEEE Conference on Decision and Control*, pp. 211–216, Los Angeles, CA, USA, Dec. 2014.
[4] A. J. Wood, B. F. Wollenberg, and G. B. Sheblé, *Power Generation, Operation, and Control*, 3rd ed. Wiley-Interscience, 2013.
[5] M. Yazdanian and A. Mehrizi-Sani, "Distributed control techniques in microgrids," *IEEE Trans. Smart Grid*, vol. 5, no. 6, pp. 2901–2909, Nov. 2014.

[6] D. K. Molzahn, F. Dörfler, H. Sandberg, S. H. Low, S. Chakrabarti, R. Baldick, and J. Lavaei, "A survey of distributed optimization and control algorithms for electric power systems," *IEEE Trans. Smart Grid*, vol. 8, no. 6, pp. 2941–2962, Nov. 2017.

[7] M. Kosari and S. H. Hosseinian, "Decentralized reactive power sharing and frequency restoration in islanded microgrid," *IEEE Trans. Power Syst.*, vol. 32, no. 4, pp. 2901–2912, Jul. 2017.

[8] J. M. Rey, P. Martí, M. Velasco, J. Miret, and M. Castilla, "Secondary switched control with no communications for islanded microgrids," *IEEE Trans. Ind. Electron.*, vol. 64, no. 11, pp. 8534–8545, Nov. 2017.

[9] M. Yazdanian and A. Mehrizi-Sani, "Washout filter-based power sharing," *IEEE Trans. Smart Grid*, vol. 7, no. 2, pp. 967–968, Mar. 2016.

[10] Y. Han, H. Li, L. Xu, X. Zhao, and J. M. Guerrero, "Analysis of washout filter-based power sharing strategy-An equivalent secondary controller for islanded microgrid without lbc lines," *IEEE Trans. Smart Grid*, vol. 9, no. 5, pp. 4061–4076, Sep. 2018.

[11] M. Castilla, A. Camacho, J. Miret, M. Velasco, and P. Martí, "Local secondary control for inverter-based islanded microgrids with accurate active power sharing under high-load conditions," *IEEE Trans. Ind. Electron.*, vol. 66, no. 4, pp. 2529–2539, Apr. 2019.

[12] E. Weitenberg, Y. Jiang, C. Zhao, E. Mallada, C. D. Persis, and F. Dörfler, "Robust decentralized secondary frequency control in power systems: Merits and trade-offs," *IEEE Trans. Autom. Control*, vol. 64, no. 10, pp. 3967–3982, Oct. 2019.

[13] A. Bidram, A. Davoudi, F. L. Lewis, and Z. Qu, "Secondary control of microgrids based on distributed cooperative control of multi-agent systems," *IET Gener. Transm. Distrib*, vol. 7, no. 8, pp. 822–831, Aug. 2013.

[14] A. Bidram, A. Davoudi, and F. L. Lewis, "A multiobjective distributed control framework for islanded AC microgrids," *IEEE Trans. Ind. Informat.*, vol. 10, no. 3, pp. 1785–1798, Aug. 2014.

[15] A. Bidram, F. L. Lewis, and A. Davoudi, "Distributed control systems for small-scale power networks: Using multiagent cooperative control theory," *IEEE Control Syst. Mag.*, vol. 34, no. 6, pp. 56–77, Dec. 2014.

[16] X. Wu and C. Shen, "Distributed optimal control for stability enhancement of microgrids with multiple distributed generators," *IEEE Trans. Power Syst.*, vol. 32, no. 5, pp. 4045–4059, Sep. 2017.

[17] G. Chen and E. Feng, "Distributed secondary control and optimal power sharing in microgrids," *IEEE/CAA Journal of Automatica Sinica*, vol. 2, no. 3, pp. 304–312, Jul. 2015.

[18] S. Zuo, A. Davoudi, Y. Song, and F. L. Lewis, "Distributed finite-time voltage and frequency restoration in islanded AC microgrids," *IEEE Trans. Ind. Electron.*, vol. 63, no. 10, pp. 5988–5997, Oct. 2016.

[19] N. M. Dehkordi, N. Sadati, and M. Hamzeh, "Distributed robust finite-time secondary voltage and frequency control of islanded microgrids," *IEEE Trans. Power Syst.*, vol. 32, no. 5, pp. 3648–3659, Sep. 2017.

[20] N. M. Dehkordi, N. Sadati, and M. Hamzeh, "Fully distributed cooperative secondary frequency and voltage control of islanded microgrids," *IEEE Trans. Energy Convers.*, vol. 32, no. 2, pp. 675–685, Jun. 2017.

[21] N. M. Dehkordi, H. R. Baghaee, N. Sadati, and J. M. Guerrero, "Distributed noise-resilient secondary voltage and frequency control for islanded microgrids," *IEEE Trans. Smart Grid*, vol. 10, no. 4, pp. 3780–3790, Jul. 2019.

[22] Y. Xu, H. Sun, W. Gu, Y. Xu, and Z. Li, "Optimal distributed control for secondary frequency and voltage regulation in an islanded microgrid," *IEEE Trans. Ind. Informat.*, vol. 15, no. 1, pp. 225–235, Jan. 2019.

[23] M. Chen, X. Xiao, and J. M. Guerrero, "Secondary restoration control of islanded microgrids with decentralized event-triggered strategy," *IEEE Trans. Ind. Informat.*, vol. 14, no. 9, pp. 3870–3880, Sep. 2018.

[24] J. Lai, H. Zhou, X. Lu, X. Yu, and W. Hu, "Droop-based distributed cooperative control for microgrids with time-varying delays," *IEEE Trans. Smart Grid*, vol. 7, no. 4, pp. 1775–1789, Jul. 2016.

[25] X. Lu, X. Yu, J. Lai, Y. Wang, and J. M. Guerrero, "A novel distributed secondary coordination control approach for islanded microgrids," *IEEE Trans. Smart Grid*, vol. 9, no. 4, pp. 2726–2740, Jul. 2018.

[26] Z. Deng, Y. Xu, H. Sun, and X. Shen, "Distributed, bounded and finite-time convergence secondary frequency control in an autonomous microgrid," *IEEE Trans. Smart Grid*, vol. 10, no. 3, pp. 2776–2788, May. 2017.

[27] Y. Xu and H. Sun, "Distributed finite-time convergence control of an islanded low-voltage AC microgrid," *IEEE Trans. Power Syst.*, vol. 33, no. 3, pp. 2339–2348, May. 2018.

[28] F. Guo, C. Wen, J. Mao, and Y. D. Song, "Distributed secondary voltage and frequency restoration control of droop-controlled inverter-based microgrids," *IEEE Trans. Ind. Electron.*, vol. 62, no. 7, pp. 4355–4364, Jul. 2015.

[29] A. Pilloni, A. Pisano, and E. Usai, "Robust finite-time frequency and voltage restoration of inverter-based microgrids via sliding-mode cooperative control," *IEEE Trans. Ind. Electron.*, vol. 65, no. 1, pp. 907–917, Jan. 2018.

[30] J. W. Simpson-Porco, F. Dörfler, and F. Bullo, "Synchronization and power sharing for droop-controlled inverters in islanded microgrids," *Automatica*, vol. 49, no. 9, pp. 2603–2611, Sep. 2013.

[31] J. W. Simpson-Porco, Q. Shafiee, F. Dörfler, J. C. Vasquez, J. M. Guerrero, and F. Bullo, "Secondary frequency and voltage control of islanded microgrids via distributed averaging," *IEEE Trans. Ind. Electron.*, vol. 62, no. 11, pp. 7025–7038, Nov. 2015.

[32] E. Tegling, M. Andreasson, J. W. Simpson-Porco, and H. Sandberg, "Improving performance of droop-controlled microgrids through distributed PI-control," in *Proc. American Control Conference (ACC)*, pp. 2321–2327, Boston, MA, USA, Jul. 2016.

[33] B. Abdolmaleki, Q. Shafiee, and H. Bevrani, "Kron reduction and L_2-stability for plug-and-play frequency control of microgrids," in *Proc. 2018 Smart Grid Conference (SGC)*, pp. 1–6, Sanandaj, Iran, Nov. 2018.

[34] B. Abdolmaleki, Q. Shafiee, A. R. Seifi, M. M. Arefi, and F. Blaabjerg, "A zeno-free event-triggered secondary control for ac microgrids," *IEEE Trans. Smart Grid*, DOI: 10.1109/TSG.2019.2945250.

[35] L. Y. Lu and C. C. Chu, "Consensus-based droop control synthesis for multiple DICs in isolated micro-grids," *IEEE Trans. Power Syst.*, vol. 30, no. 5, pp. 2243–2256, Sep. 2015.

[36] Q. Shafiee, V. Nasirian, J. C. Vasquez, J. M. Guerrero, and A. Davoudi, "A multi-functional fully distributed control framework for AC microgrids," *IEEE Trans. Smart Grid*, vol. 9, no. 4, pp. 3247–3258, Jul. 2018.

[37] B. Abdolmaleki, Q. Shafiee, M. M. Arefi, and T. Dragičević, "An instantaneous event-triggered hz-watt control for microgrids," *IEEE Trans. Power Syst.*, vol. 34, no. 5, pp. 3616–3625, Sep. 2019.

[38] Q. Shafiee, J. M. Guerrero, and J. C. Vasquez, "Distributed secondary control for islanded microgrids–A novel approach," *IEEE Trans. Ind. Electron.*, vol. 29, no. 2, pp. 1018–1031, Feb. 2014.

[39] Q. Shafiee, Č. Stefanović, T. Dragičević, P. Popovski, J. C. Vasquez, and J. M. Guerrero, "Robust networked control scheme for distributed secondary control of islanded microgrids," *IEEE Trans. Ind. Electron.*, vol. 61, no. 10, pp. 5363–5374, Oct. 2014.

[40] S. Riverso, M. Tucci, J. C. Vasquez, J. M. Guerrero, and G. Ferrari-Trecate, "Stabilizing plug-and-play regulators and secondary coordinated control for AC islanded microgrids with bus-connected topology," *Applied Energy*, vol. 6, pp. 914–924, Jan. 2018.

[41] W. Ren, R. W. Beard, and E. M. Atkins, "Information consensus in multivehicle cooperative control," *IEEE Control Syst. Mag.*, vol. 27, no. 2, pp. 71–82, Apr. 2007.

[42] R. Olfati-Saber, J. A. Fax, and R. M. Murray, "Consensus and cooperation in networked multi-agent systems," *Proc. IEEE*, vol. 95, no. 1, pp. 215–233, Jan. 2007.

[43] D. P. Spanos, R. Olfati-Saber, and R. M. Murray, "Dynamic consensus on mobile networks," in *Proc. 16th IFAC World Congress*, Prague, Czech Republic, 2005.

[44] I. U. Nutkani, P. C. Loh, and F. Blaabjerg, "Droop scheme with consideration of operating costs," *IEEE Trans. Power Electron.*, vol. 29, no. 3, pp. 1047–1052, Mar. 2014.

[45] I. U. Nutkani, P. C. Loh, P. Wang, and F. Blaabjerg, "Cost-prioritized droop schemes for autonomous AC microgrids," *IEEE Trans. Power Electron.*, vol. 30, no. 2, pp. 1109–1119, Feb. 2015.

[46] I. U. Nutkani, P. C. Loh, P. Wang, and F. Blaabjerg, "Linear decentralized power sharing schemes for economic operation of AC microgrids," *IEEE Trans. Ind. Electron.*, vol. 63, no. 1, pp. 225–234, Jan. 2016.

[47] I. U. Nutkani, P. C. Loh, P. Wang, and F. Blaabjerg, "Decentralized economic dispatch scheme with online power reserve for microgrids," *IEEE Trans. Smart Grid*, vol. 8, no. 1, pp. 139–148, Jan. 2017.

[48] A. Elrayyah, F. Cingoz, and Y. Sozer, "Construction of nonlinear droop relations to optimize islanded microgrid operation," *IEEE Trans. Ind. Appl.*, vol. 51, no. 4, pp. 3404–3413, Jul. 2015.

[49] F. Cingoz, A. Elrayyah, and Y. Sozer, "Plug-and-play nonlinear droop construction scheme to optimize islanded microgrid operations," *IEEE Trans. Power Electron.*, vol. 32, no. 4, pp. 2743–2756, Apr. 2017.

[50] F. Chen, M. Chen, Q. Li, K. Meng, Y. Zheng, J. M. Guerrero, and D. Abbott, "Cost-based droop schemes for economic dispatch in islanded microgrids," *IEEE Trans. Smart Grid*, vol. 8, no. 1, pp. 63–74, Jan. 2017.

[51] H. Han, L. Li, L. Wang, M. Su, Y. Zhao, and J. M. Guerrero, "A novel decentralized economic operation in islanded AC microgrids," *Energies*, vol. 10, no. 6, Jun. 2017.

[52] S. Yang, S. Tan, and J.-X. Xu, "Consensus based approach for economic dispatch problem in a smart grid," *IEEE Trans. Power Syst.*, vol. 28, no. 4, pp. 4416–4426, Nov. 2013.

[53] C. Zhao, X. Duan, and Y. Shi, "Analysis of consensus-based economic dispatch algorithm under time delays," *IEEE Trans. Syst. Man Cybern. Syst.*, DOI: 10.1109/TSMC.2018.2840821.
[54] T. Yang, D. Wu, Y. Sun, and J. Lian, "Minimum-time consensus-based approach for power system applications," *IEEE Trans. Ind. Electron.*, vol. 63, no. 2, pp. 1318–1328, Feb. 2016.
[55] G. Chen, J. Ren, and E. N. Feng, "Distributed finite-time economic dispatch of a network of energy resources," *IEEE Trans. Smart Grid*, vol. 8, no. 2, pp. 822–832, Mar. 2017.
[56] G. Chen and Z. Zhao, "Delay effects on consensus-based distributed economic dispatch algorithm in microgrid," *IEEE Trans. Power Syst.*, vol. 33, no. 1, pp. 602–612, Jan. 2018.
[57] H. Xin, L. Zhang, Z. Wang, D. Gan, and K. P. Wong, "Control of island AC microgrids using a fully distributed approach," *IEEE Trans. Smart Grid*, vol. 6, no. 2, pp. 943–945, Mar. 2015.
[58] X. Wu, C. Shen, and R. Iravani, "A distributed, cooperative frequency and voltage control for microgrids," *IEEE Trans. Smart Grid*, vol. 9, no. 4, pp. 2764–2776, Jul. 2018.
[59] X. Zhou and Q. Ai, "A distributed economic control and transition between economic and non-economic operation in islanded microgrids," *Electric Power Systems Research*, vol. 158, pp. 70–81, May. 2018.
[60] F. Dörfler and S. Grammatico, "Gather-and-broadcast frequency control in power systems," *Automatica*, vol. 79, pp. 296–305, May. 2017.
[61] F. Dörfler and F. Bullo, "Kron reduction of graphs with applications to electrical networks," *IEEE Trans. Circuits Syst. I*, vol. 60, no. 1, pp. 150–163, Jan. 2013.
[62] K. Fitch, "Effective resistance preserving directed graph symmetrization," *SIAM Journal on Matrix Analysis and Applications*, vol. 40, no. 1, pp. 49–65, 2019.
[63] A. Yazdani and R. Iravani, *Voltage-Sourced Converters in Power Systems: Modeling, Control, and Applications*. John Wiley & Sons, 2010.
[64] M. B. Delghavi, S. Shoja-Majidabad, and A. Yazdani, "Fractional-order sliding-mode control of islanded distributed energy resource systems," *IEEE Trans. Sustain. Energy*, vol. 7, no. 4, pp. 1482–1491, Oct. 2016.
[65] T. Dragičević, "Model predictive control of power converters for robust and fast operation of AC microgrids," *IEEE Trans. Power Electron.*, vol. 33, no. 7, pp. 6304–6317, Jul. 2018.
[66] J. Schiffer, R. Ortega, A. Astolfi, J. Raisch, and T. Sezi, "Conditions for stability of droop-controlled inverter-based microgrids," *Automatica*, vol. 50, no. 10, pp. 2457–2469, Oct. 2014.
[67] X. Wu, C. Shen, and R. Iravani, "Feasible range and optimal value of the virtual impedance for droop-based control of microgrids," *IEEE Trans. Smart Grid*, vol. 8, no. 3, pp. 1242–1251, May. 2017.
[68] H. Lin and P. J. Antsaklis, "Stability and stabilizability of switched linear systems: A survey of recent results," *IEEE Trans. Autom. Control*, vol. 54, no. 2, pp. 308–322, Feb. 2009.
[69] F. L. Lewis, D. M. Dawson, and C. T. Abdallah, *Robot Manipulator Control: Theory and Practice*. CRC Press, 2003.
[70] R. A. Horn and C. R. Johnson, *Matrix Analysis*. Cambridge University Press, 2012.
[71] E. Fridman, *Introduction to time-delay systems: Analysis and control*. Springer, 2014.

Babak Abdolmaleki (S'17-M'18) was born in Kurdistan, Iran, in 1992. He received the B.Sc. and M.Sc. degrees in electrical engineering from Shiraz University, Shiraz, Iran, in 2014 and 2017, respectively.

Since 2017, he has been a Research Associate with the Smart/Micro Grids Research Center, University of Kurdistan, Sanandaj, Iran. His main research interests are centered around distributed optimization and control, event-triggered control, advanced control of power converters, and modern power systems dynamics and control.

Qobad Shafiee (S'13-M'15-SM'17) received the Ph.D. degree in electrical engineering from the Department of Energy Technology, Aalborg University, Denmark, in 2014.

He is currently an Assistant Professor, an Associate Director of International Relations, and the Program Co-Leader of the Smart/Micro Grids Research Center with the University of Kurdistan, Sanandaj, Iran, where he was a Lecturer from 2007 to 2011. In 2014, he was a Visiting Scholar with the Electrical Engineering Department, University of Texas at Arlington, Arlington, TX, USA. In 2015, he was a Post-Doctoral Fellow with the Department of Energy Technology, Aalborg University. His current research interests include modeling, energy management, control of power electronics-based systems and microgrids, and model predictive and optimal control of modern power systems.